Investigation of Nanocrystalline Materials by Perturbed Angular Correlation and Supplementing Experimental Techniques

H. WOLF

Technische Physik, Universität des Saarlandes
66123 Saarbrücken, Germany

Nanocrystalline materials were investigated by perturbed $\gamma\gamma$-angular correlation using the radioactive probe ^{111}In. For identifying local structures observed by perturbed $\gamma\gamma$-angular correlation various supplementing experimental techniques, like X-ray diffraction, transmission electron microscopy, absorption spectroscopy, and photoluminescence spectroscopy, were applied. In nanocrystalline TiAl alloys different crystallographic structures were observed depending on the conditions of sample treatment. Nanocrystalline Ni samples show a slightly modified local magnetic field in regions adjacent to the grain boundaries. In addition, ordered grain boundary structures were observed. Ni precipitates were identified in nanocrystalline NiCu alloys by perturbed $\gamma\gamma$-angular correlation and preparation conditions avoiding these precipitates were found. For nanocrystalline ZnO preparation conditions were found yielding In-doped particles of good crystalline quality.

PACS numbers: 68.35.Ct, 75.75.+a, 78.67.Bf, 81.07.Bc, 82.45.Qr

1. Introduction

The properties of nanocrystalline materials are essentially determined by grain size and properties of the grain boundaries of the respective material [1]. Using perturbed $\gamma\gamma$-angular correlation (PAC) valuable information about local crystalline structures of the grains or the grain boundaries is obtained. PAC detects the hyperfine interaction of the nucleus of a suitable radioactive probe atom, here ^{111}In, decaying to ^{111}Cd, with an electric field gradient (EFG) or magnetic field. The hyperfine interaction is detected by recording the γ–γ cascade, which is emitted after the radioactive decay of the probe nucleus, in delayed coincidence. The hyperfine interaction causes a modulation of the exponential decay function of the intermediate level of the γ–γ cascade. The modulation function $R(t)$ is governed by a frequency triplet in case of an electric quadrupole interaction,

$$R(T) = A_2 \left(s_0 + \sum_{n=1}^{3} s_n \cos(\omega_n t) \right), \tag{1}$$

where A_2 is the anisotropy coefficient of the $\gamma-\gamma$ cascade. For the frequencies the relation $\omega_1 + \omega_2 = \omega_3$ holds, the magnitude of the frequency ω_1 is determined by the strength of the local EFG, which usually is expressed by the quadrupole coupling constant $\nu_Q \sim \omega_1 \sim V_{zz}$. The ratio ω_2/ω_1 is determined by the asymmetry parameter $\eta = (V_{xx} - V_{yy})/V_{zz}$ of the EFG tensor. In case of a magnetic dipole interaction the modulation is governed by a frequency doublet,

$$R(T) = A_2 \left(s_0 + \sum_{n=1}^{2} s_n \cos(n\omega_{\mathrm{L}} t) \right), \tag{2}$$

where the Larmor frequency ω_{L} is proportional to the strength of the local magnetic field. If several, non-equivalent lattice sites are occupied by the probe atoms, the modulation function is split into different fractions,

$$R(t) = \sum_{i} f_i R_i(t) \quad \text{with} \quad \sum_{i} f_i = 1, \tag{3}$$

each characterized by their own frequency triplet or doublet, working like a fingerprint of the corresponding local structure. More details about PAC and its applications can be found in [2–4].

2. Results and discussion

For PAC investigations the samples have to be doped with radioactive ^{111}In atoms. Depending on the method of preparation the probe atoms are distributed evenly over the sample, or, in special cases, preferably placed into the grain boundaries. By annealing nanocrystalline materials, new crystalline phases might be formed, which can be detected by PAC measurements. For an assignment of the respective PAC signal to a distinct local lattice structure, in general, investigations by supplementing experimental techniques are necessary. In the following, some examples will be discussed showing the versatility of information obtainable by PAC investigations.

2.1. Phase formation in TiAl alloys

Nanocrystalline TiAl alloys were prepared by ball milling using a standard Spex 8000 ball mill. For this purpose, powders of Ti (purity 99.98%) and of Al (99.99%) with particle sizes smaller than 150 μm were mixed and filled into hardened steel vials under Ar atmosphere. The milling times ranged between 2 h and 52 h. Subsequently, ^{111}In atoms were diffused into the sample at 690 K in an evacuated quartz ampoule. PAC spectra were also taken after ^{111}In diffusion under additional annealing at various temperatures up to 1060 K. PAC data from samples of composition $Ti_{0.5}Al_{0.5}$ are shown in Fig. 1 for a milling time of 4 h and in Fig. 2 for a milling time of 13 h. After diffusion of ^{111}In no ordered structure is observed by PAC (see Fig. 2, top panel), while X-ray diffraction (XRD) investigations show the signature of a *hcp* structure. After annealing at 880 K the PAC data of
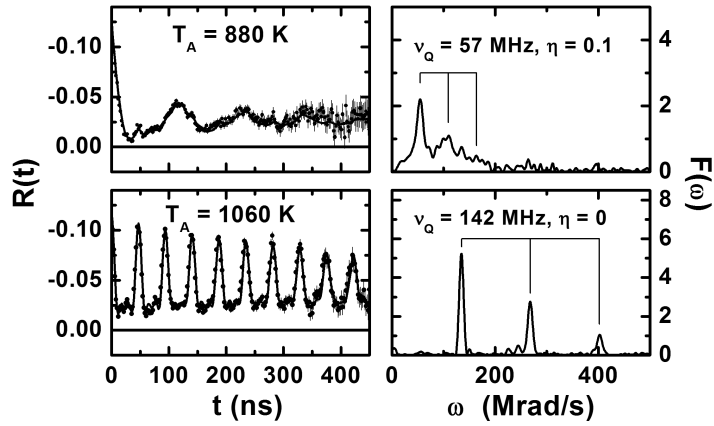
Fig. 1. PAC spectra of a $Ti_{0.5}Al_{0.5}$ sample after 4 h milling time. The alloy was diffused with the ^{111}In probe atoms at 690 K and subsequently annealed at 880 K (top panel) and 1060 K (bottom panel).

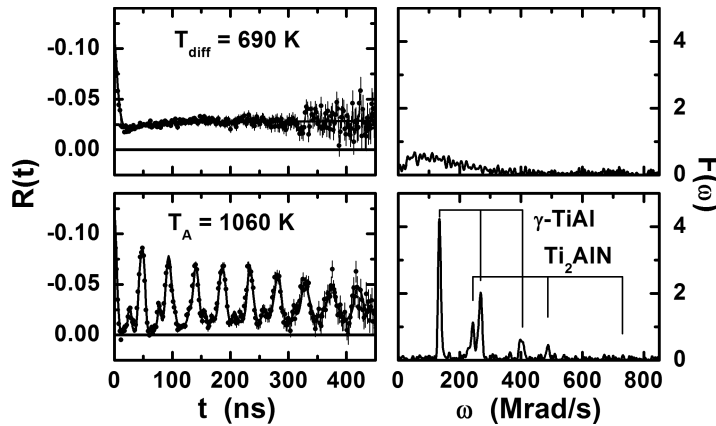Fig. 2. PAC spectra of a $Ti_{0.5}Al_{0.5}$ sample after 13 h milling time. The alloy was diffused with the ^{111}In probe atoms at 690 K (top panel) and subsequently annealed at 1060 K (bottom panel).

the sample milled for 4 h show an EFG distribution about 57 MHz (Fig. 1, top panel), which is not known from elemental Ti or Al samples. At the same time, XRD investigations just show the *fct* structure characteristic of a $Ti_{0.5}Al_{0.5}$ alloy. Increasing the annealing temperature to 1060 K, the PAC data show a unique EFG of 142 MHz (Fig. 1, bottom panel), which is known to be caused by the intermetallic compound TiAl [5], while the XRD data remain almost unchanged. Annealing the sample milled for 13 h at 1060 K, besides the intermetallic compound γ-TiAl an additional crystalline structure is observed by PAC ($\nu_Q = 257$ MHz, see Fig. 2, bottom panel), which on the basis of XRD data is identified as Ti_2AlN. The longer milling time obviously leads to enhanced incorporation of N impurities

into the Ti–Al alloy. More details about the investigations of Ti–Al alloys can be found in Ref. [6].

2.2. Magnetic boundaries in nanocrystalline Ni

Nanocrystalline Ni was prepared by pulsed electrodeposition (PED) [7]. Short current pulses with a length of $t_{on} = 2$ ms and a current density of 1 A/cm^2 were applied followed by an off-time of 48 ms. The electrolyte used for deposition consisted of Ni(II)sulfate (40 g/l), K, Na-tartrate (120 g/l), and ammonium chloride (40 g/l). The average grain size is controlled by the current density, by the temperature of the electrolyte, and by the optional addition of saccharin. For doping of nanocrystalline Ni samples *in situ* with ^{111}In, radioactive ^{111}InCl$_3$ was added to the electrolyte. The average grain size of the nanocrystalline Ni samples was determined by XRD.
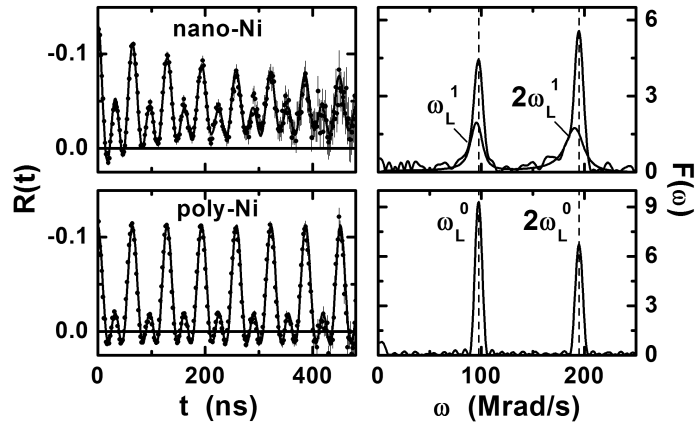

Fig. 3. PAC spectrum of nanocrystalline Ni (top panel) compared to polycrystalline Ni (bottom panel).

The PAC spectrum plotted in Fig. 3 shows primarily the magnetic dipole interaction of ferromagnetic Ni. A detailed analysis yields that the PAC spectrum consists of two components (top panel). The first one exhibits the sharp Larmor frequency $\omega_L^0 = 97.6$ Mrad/s known from polycrystalline Ni (bottom panels) and caused by the ferromagnetism of Ni. The second component is shifted to a somewhat lower frequency of $\omega_L^1 = 95.8$ Mrad/s and is accompanied by a significant frequency distribution of $\Delta\omega_L^1 = 6$ Mrad/s. Due to the preparation conditions it can be assumed that the ^{111}In atoms are homogeneously distributed in the sample. It is suggested, therefore, that the ^{111}In atoms exposed to the slightly modified local magnetic field are located near the grain boundaries. Using the relative fractions of about $f_0 = 49\%$ corresponding to ω_L^0 and $f_1 = 37\%$ corresponding to ω_L^1, and the average particle size of about 40 nm, as determined by XRD, it is estimated that the width of the layer corresponding to the modified local magnetic field is

of the order of 3–4 nm. This so-called magnetic boundary is significantly larger than the crystallographic boundary of about only 1 nm. A detailed description of these experiments can be found in [8].

2.3. Ordered grain boundary structures in nanocrystalline Ni

The diffusion of ^{111}In atoms into nanocrystalline Ni takes place at significantly lower temperatures than into polycrystalline Ni. The PAC data plotted in Fig. 4, obtained after diffusion at 673 K (top panel), do not show the magnetic interaction known from bulk Ni. Rather, a fraction of about 10% of the probe atoms shows the signature of an electric quadrupole interaction. Increasing the temperature to 823 K (middle panel) different signals originating from different well-defined electric field gradients are observed, but still no unique magnetic interaction. After annealing at 1073 K (bottom panel), both another EFG signal and the signal of the magnetic hyperfine interaction known from bulk Ni are observed.
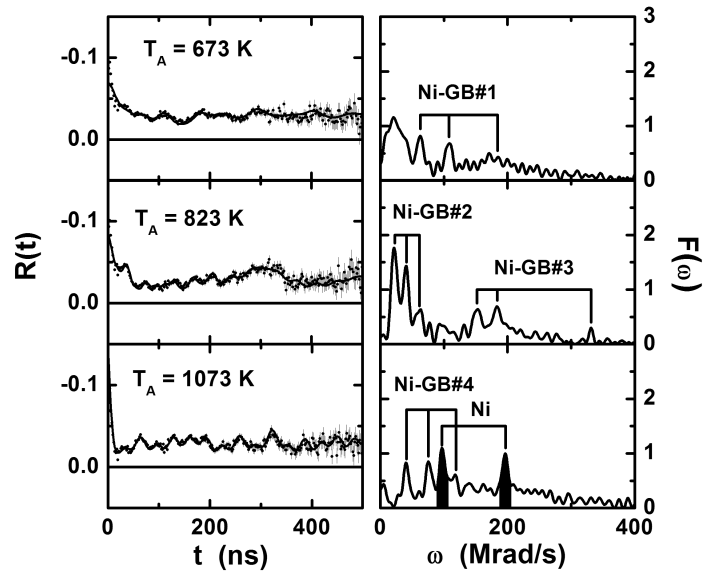

Fig. 4.   Ordered grain boundary structures in Ni detected by PAC.

The diffusion of ^{111}In at temperatures below about 1000 K is determined predominantly by diffusion along grain boundaries [9]. From the PAC data it is concluded that in the grain boundaries obviously no unique magnetic field exists. The presence of sharp EFG signals, however, indicates that there exist ordered structures in the grain boundaries of Ni. Above 1000 K also the volume diffusion of In becomes important, and a measurable fraction of the ^{111}In probe atoms diffuses from the grain boundaries into the crystallites as is shown by the characteristic magnetic hyperfine field. At present, four different ordered grain boundary structures have been detected by PAC [10]. It should be noted that there is no other

experimental technique able to detect ordered grain boundary structures, with the exception of high resolution electron microscopy, which was successfully applied for the detection of ordered grain boundary structures in NiO bicrystals [11].

2.4. Homogeneity of NiCu alloys

Nanocrystalline Ni–Cu alloys were prepared by PED, using an electrolyte consisting of $NiSO_4$, $CuSO_4$, and Na-citrate. Optionally, saccharin was added to the electrolyte. For doping the Ni–Cu nanoparticles with ^{111}In, [111]$InCl_3$ was added to the electrolyte. Since the deposition of Cu is much more effective than of Ni, the atomic ratio of Ni and Cu in the electrolyte had to be around 13 in order to prepare a Ni–Cu alloy with an atomic ratio of 1. Particle size and homogeneity of the alloy depend on the temperature of the electrolyte, the current density during electro deposition, and on the addition of saccharin to the electrolyte. If no saccharin is added to the electrolyte, the Fourier spectra of the PAC data displayed in Fig. 5 clearly show the presence of Ni precipitates as indicated by the Larmor frequency corresponding to ^{111}In atoms being substitutionally incorporated in bulk
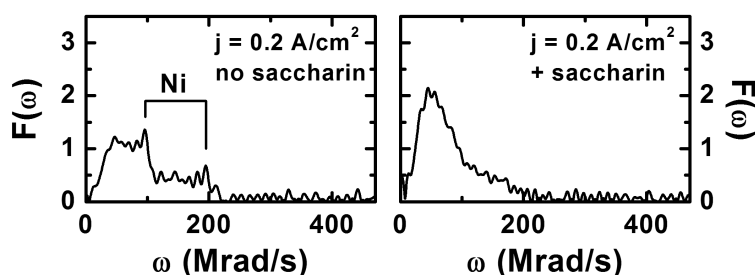

Fig. 5. Ni precipitates observed in a nanocrystalline NiCu alloy by PAC (left panel). Adding saccharin to the electrolyte (right panel) avoids the precipitation of Ni.

Ni (left panel) as shown by the absence of the respective Larmor frequency. The Ni precipitates disappear if saccharin is added during deposition (right panel). The Ni precipitates cannot be identified on the basis of XRD data, showing the excellent sensitivity of PAC to the formation of these precipitates. More information about the investigations of nanocrystalline NiCu alloys can be found in Ref. [12].

2.5. In donors in ZnO

Nano ZnO was prepared by the electrochemical deposition under oxidizing conditions (EDOC) method [13]. The electrolysis process uses two Zn electrodes and takes place in a solution of 0.1 M tetrabutylammonium-bromide (TBA-Br) dissolved in 2-propanol. The nanocrystalline ZnO samples were doped *in situ* with radioactive ^{111}In by diffusing the ^{111}In dopants into the sacrificial electrode before electrolysis. After preparation, a hydrothermal treatment at temperatures between 373 K and 523 K was applied to the ZnO nanocrystals. More details about the EDOC method and the hydrothermal treatment are given in [14]. The

incorporation of In atoms on substitutional lattice sites is determined by PAC if the EFG due to the hexagonal lattice structure of ZnO, which is known from bulk ZnO [15], is detected. The ZnO nanocrystals were investigated in parallel by transmission electron microscopy and XRD in order to determine shape, size, size distribution, and microstrain of the particles, and by absorption and photoluminescence spectroscopy in order to determine their optical properties.

Comprehensive investigations show that after hydrothermal annealing at 473 K the average size of the spherical particles is increased from 4 nm to 11 nm; at the same time the microstrain present after deposition disappears. Furthermore, the absorption power and the excitonic emission after laser excitation are increased. The PAC investigations displayed in Fig. 6 show no detectable fraction directly after deposition (top panel) but after hydrothermal treatment at 473 K about 20% of the ^{111}In atoms were incorporated on substitutional Zn sites (bottom panel). Increasing the annealing temperature to 523 K the optical properties
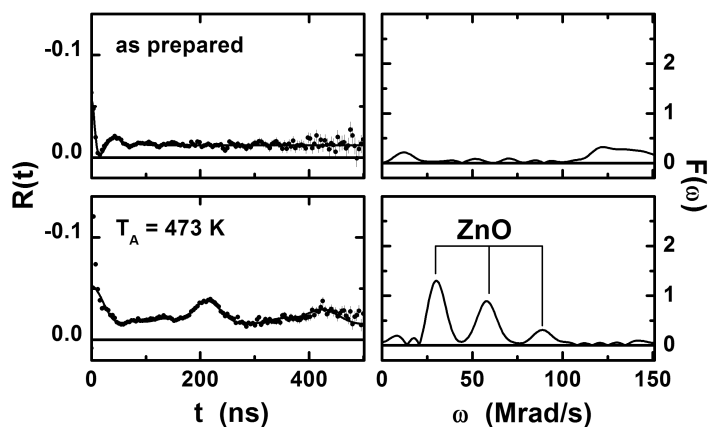

Fig. 6. PAC spectra of nanocrystalline ZnO after deposition (top panels) and after subsequent hydrothermal annealing at 473 K (bottom panels). The modulation caused by an EFG shows the incorporation of ^{111}In atoms on substitutional Zn sites.

changed only slightly and the fraction of ^{111}In atoms on substitutional Zn sites was slightly increased. The particles, however, have grown significantly into about 200 nm long rod-shaped crystals. Thus, the temperature of 473 K was identified as being an optimum for producing ZnO nanocrystals of good crystalline quality doped with In atoms on substitutional lattice sites. The full description of the experimental analysis of nanocrystalline ZnO is found in Ref. [14].

3. Summary

The investigations of nanocrystalline materials by PAC yield valuable, in part unique, information about crystallites and grain boundaries. It turned out that in some cases the sensitivity of PAC to phenomena, like ordered grain boundary

structures or precipitates in alloys, is much higher than that of other experimental techniques. By PAC investigations the donor-like incorporation of In atoms into ZnO nanocrystals was shown.

Acknowledgments

References

[1] H. Gleiter, *Prog. Mater. Sci.* **33**, 223 (1989).

[2] G. Schatz, A. Weidinger, *Nuclear Condensed Matter Physics*, Wiley, Chichester (England) 1995, p. 63.

[3] Th. Wichert, E. Recknagel in: *Topics in Current Physics*, Ed. U. Gonser, Vol. 40, Berlin 1986, p. 317.

[4] Th. Wichert, in: *Identification of Defects in Semiconductors*, Ed. M. Stavola, Academic Press, London 1999, p. 297.

[5] J. Fan, G.S. Collins, *Hyp. Int.* **79**, 745 (1993).

[6] St. Lauer, Z. Guan, H. Wolf, Th. Wichert, *J. Mater. Res.* **17**, 2130 (2002).

[7] H. Natter, M. Schmelzer, R. Hempelmann, *J. Mater. Res.* **13**, 1186 (1998).

[8] St. Lauer, Z. Guan, H. Wolf, H. Natter, M. Schmelzer, R. Hempelmann, Th. Wichert, *Nanostruct. Mater.* **12**, 955 (1999).

[9] I. Kaur, W. Gust, L. Kozma, *Handbook of Grain and Interphase Boundary Diffusion Data*, Ziegler Press, Stuttgart 1989, p. 1003.

[10] Z. Guan, H. Wolf, X. Li, Th. Wichert, *Hyp. Int.* **136/137**, 281 (2001); Z. Guan, H. Wolf, X. Li, Th. Agne, Th. Wichert, in preparation for publication.

[11] K.L. Merkle, J.F. Reddy, C.L. Willy, D.J. Smith, *Phys. Rev. Lett.* **59**, 2887 (1987).

[12] H. Wolf, Z. Guan, St. Lauer, H. Natter, M. Schmelzer, R. Hempelmann, Th. Wichert, *J. Metast. Nanocryst. Mater.* **8**, 847 (2000).

[13] A. Dierstein, H. Natter, F. Meyer, H.-O. Stephan, Ch. Kropf, R. Hempelmann, *Scr. Mater.* **44**, 2209 (2001).

[14] Th. Agne, Z. Guan, R. Hempelmann, X. Li, H. Natter, H. Wolf, Th. Wichert, *Appl. Phys. Lett.* **83**, 1204 (2003).

[15] H. Wolf, S. Deubler, D. Forkel, H. Foettinger, M. Iwatschenko-Borho, F. Meyer, M. Renn, W. Witthuhn, R. Helbig, *Mater. Sci. Forum* **10-12**, 863 (1986).